Int. J. Electrochem. Sci., 11 **(2016)** 6609 – 6626, doi: 10.20964/2016.08.17

International Journal of ELECTROCHEMICAL SCIENCE
www.electrochemsci.org

Evaluation of Inhibition Efficiency of 1-(2-pyridylazo) -2-naphthol and Bromide Ion on the Corrosion of Mild Steel in Sulphuric Acid Solution

Lin Wang[1,*], *Hao Zheng*[1], *Xue-Min Zi*[2], *Shi-Wen Zhang*[1], *Li Peng*[1], *Jie Xiong*[1]

[1] School of Chemical Science and Technology, Key Laboratory of Medicinal Chemistry for Nature Resource, Ministry of Education, Yunnan University, Kunming, Yunnan, 650091, P. R. China
[2] Yunnan Three Circles-Sinochem Fertilizers Co. Ltd, Kunming, Yunnan, 650114, P. R. China
[*]E-mail: wanglin@ynu.edu.cn, wanglin2812@163.com

Received: 11 April 2016 / *Accepted:* 25 May 2016 / *Published:* 7 July 2016

The corrosion inhibition of mild steel in 0.5 mol/L sulphuric acid solution by bromide ion in the absence and presence of 1-(2-pyridylazo)-2-naphthol (PAN) has been studied by potentiodynamic polarization, electrochemical impedance spectroscopy and weight loss. Potentiodynamic polarization researches show that single bromide ion or the complex of bromide ion and PAN acts as a mixed-type inhibitor and do not change the mechanism of either hydrogen evolution reaction or metal dissolution. The charge transfer process controls the corrosion reaction. The studies reveal that the complex of bromide ion and PAN shows a quite well inhibition and their synergistic effect was observed and discussed. The adsorption of the inhibitors on the steel surface obeys the Langmuir adsorption isotherm. The thermodynamic parameters such as adsorptive equilibrium constant (K_{ads}), adsorption free energy (ΔG^{o}_{ads}), adsorption heat (ΔH^{o}_{ads}) and adsorption entropy (ΔS^{o}_{ads}), kinetic data such as apparent activation energy (E_a) and pre-exponential factor (A) were calculated and discussed. The values of ΔG^{o}_{ads} indicate that the adsorption of the inhibitors on the mild steel surface in 0.5 mol/L H_2SO_4 solution is a mixed physical and chemical adsorption mechanism and the chemical adsorption is the dominant in the presence of bromide ion and PAN together.

Keywords: Corrosion inhibition, Mild steel, Electrochemical techniques, Adsorption, Thermodynamic properties, Synergistic effect, Sulphuric acid.

1. INTRODUCTION

Acid solutions are generally used for removal of undesirable scale and rust in several industrial processes. The wide use of hydrochloric and sulphuric acids during pickling and industrial cleaning may cause metal corrosion and lead to economic losses [1-2]. The use of inhibitors is one of the most

practical methods for protection against corrosion, especially in acidic media [3-6]. Most of the acid inhibitors are organic compounds containing nitrogen [7-12], sulphur [5,13-16] and oxygen [17-19] atoms. Compounds with π-electrons and functional groups containing heteroatoms which can donate lone pair electrons are found to be particularly useful as inhibitors for corrosion of metals [4,20-23]. A number of different type organic compounds are known to be applicable as corrosion inhibitors for steel in acidic solution [24-28]. Some researches show that nitrogen-containing organic inhibitors have better inhibition for the steel corrosion in hydrochloric acid (HC) than in sulphuric acid (H_2SO_4) [29-30]. The possible reason is that chloride ions (Cl^-) and nitrogen-containing organic inhibitors have a synergistic inhibition for steel corrosion in HCl. Some studies about synergism between Cl^- and organic compounds on metal corrosion in acidic solution have been reported [31-33]. Synergism is a combined action of compounds and it is generally observed that the addition of chloride ions to the corrosive media increases the adsorption ability of organic cations by forming interconnecting bridges between negatively charged metal surface and inhibitor cations [34-37]. Synergism is an effective means of improving the inhibitive forces of the inhibitors with respect to using as a single inhibitor. Synergistic effect has been frequently used in practice for its efficiency and economy [31, 38-39].

1-(2-pyridylazo) -2-naphthol (PAN) can be as an indicator. It has abundant π-electrons heterocyclic and nitrogen atoms unshared electron pairs. Tang et al studied the inhibition of PAN and Cl^- for the steel corrosion in H_2SO_4 solution [36]. The results indicated that there was a synergistic inhibition between PAN and Cl^- for the steel corrosion in H_2SO_4 solution, but higher Cl^- concentration was used in experiment. Bromine and chlorine are the adjacent elements of the same main group. There is a bigger radius bromide ion than chloride ion. Since it has better steric effect and easy polarizability, Br^- ions should be adsorbed on metal surface and provide better synergistic effect [37].

This paper attempts to deal with the study of the synergistic inhibition effect of mild steel corrosion in H_2SO_4 solution by bromide ion and 1-(2-pyridylazo) -2-naphthol using polarization, impedance techniques and weight loss. The isotherm was applied for the testing in describing the adsorption behavior and adsorption mechanisms of the inhibitors were investigated. We attempt to acquire the higher synergistic inhibition efficiency using lower concentrations of PAN and Br^-.

2. EXPERIMENTAL

2.1. Materials

The mild steel used in this study has the following chemical composition (wt%): 0.10% C, 0.017% S, 0.026% P, 0.28% Mn, 0.050% Si and Fe remainder.

All solutions were prepared from bidistilled water and AR grade H_2SO_4 and potassium bromide (KBr) were used. PAN was supplied by Merck Chemicals. The molecular structure of PAN is shown in Figure 1.

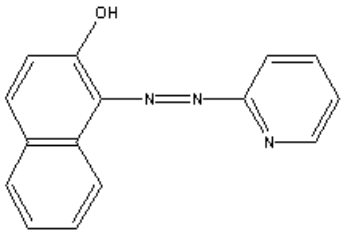

Figure 1. Structure of PAN.

2.2. Electrochemical measurements

Electrochemical measurement were carried out in a three-electrode cell containing 250 mL testing solution including a working electrode, an auxiliary electrode and a reference electrode. The mild steel used as working electrode is exposed surface of 1.0 cm^2 embedded in PVC holder by epoxy resin. Before each experiment, the working electrode was polished with a series of emery papers from 100 to 1200 grade. After polishing, the electrode was washed with distilled water, degreased with acetone, and dried with a warm air stream. The auxiliary electrode was a platinum foil and the reference electrode is saturate calomel electrode (SCE) with Luggin capillary positioned close to the working electrode surface in order to minimize ohmic potential drop. Before measurements the working electrodes were immersed in the testing solution at open circuit potential for 2 hours until a steady state was obtained.

All the electrochemical measurements were carried out by PARSTAT 2263 Potentiostat/Galvanostat (Princeton Applied Research). The Tafel polarization curves were obtained in the range of potential from -250mV to + 250mV versus open circuit potential with a scan rate of 0.5 mVs^{-1}. The electrochemical impedance spectroscopy (EIS) was carried out in a frequency range of 100 kHz to 0.01 Hz with a 10 mV peak to peak voltage excitation.

2.3. Gravimetric measurements

The specimens of mild steel with dimensions (40 mm × 15 mm × 0.4 mm) were used during the weight loss measurements. The samples were prepared by abrading with a series of emery paper from 100 to 1200 grades and washed in distilled water, degreased in acetone, dried in a stream of air.

After weighing accurately, the specimens were immersed in testing solutions (200 mL) for 4 hours in air without bubbling. At the end of the experiment the specimens were taken out, washed with distilled water and acetone, dried and immediately weighed accurately.

3. RESULTS AND DISCUSSION

3.1. Polarization measurements

The inhibition efficiency could be calculated from corrosion current density using the following formula [40]:

$$IE = \frac{I^0_{corr} - I^{inh}_{corr}}{I^0_{corr}} \times 100 \qquad (1)$$

where I^0_{corr} and I^{inh}_{corr} are the corrosion current density values in the absence and presence of inhibitors, respectively.

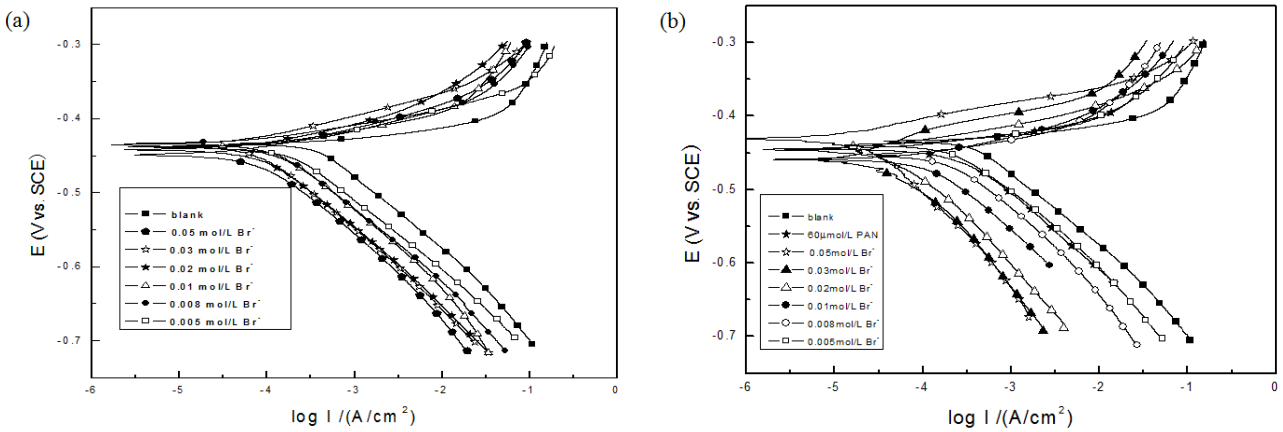

Figure 2. Polarization curves for mild steel in 0.5 mol/L H_2SO_4 containing different concentrations of Br^- in the absence (a) and presence (b) of 60 μmol/L PAN at 25 °C.

Table 1. Tafel polarization parameters and inhibition efficiencies for mild steel in 0.5 mol/L H_2SO_4 in the absence and presence of different concentration of inhibitors at 25 °C.

Br^- (mol/L)	PAN (μmol/L)	$-E_{corr}$ (vs SCE) (mv)	I_{corr} (μA/cm^2)	$-\beta_c$ (mV/dec)	β_a (mV/dec)	IE (%)
0	0	437.3	340.9	101.3	44.88	-
0.005	0	430.4	220.4	95.77	38.37	35.4
0.008	0	437.7	215.3	121.6	46.78	36.8
0.01	0	438.4	212.6	93.88	41.21	37.6
0.02	0	442.1	203.0	104.2	24.34	40.5
0.03	0	425.2	201.6	111.9	36.81	40.9
0.05	0	458.1	128.5	106.4	33.07	62.3
0	60	442.0	186.5	100.7	36.77	45.3
0.005	60	440.5	61.10	109.3	25.44	82.1
0.008	60	452.7	60.50	112.9	42.48	82.3
0.01	60	459.4	53.50	107.2	34.42	84.3
0.02	60	439.4	47.10	121.5	31.67	86.2
0.03	60	460.5	39.00	96.39	20.90	88.6
0.05	60	433.0	21.90	89.00	35.34	93.6

The polarization curves for mild steel at different concentrations of Br^- without and with 60 μmol/L PAN in 0.5 mol/L H_2SO_4 at 25°C are shown in Figure 2. It is seen from Figure 2(a), the presence of single Br^- slightly shifts the corrosion potential to both positive and negative directions. The cathodic and anodic branches are also shifted to negative or positive potential directions, These results indicate that Br^- in H_2SO_4 acts as a mixed type inhibitor. From Figure 2(b), when 60 μmol/L PAN was added, the shifts of cathodic and anodic branches are similar to those in the absence of PAN but the shifting levels are obviously larger and the cathodic branches are more clearly shifted to negative potential direction, indicating that retarding the cathodic reaction is more dominant. These results mean that the combination of Br^- and PAN in H_2SO_4 acts as a mixed type inhibitor too.

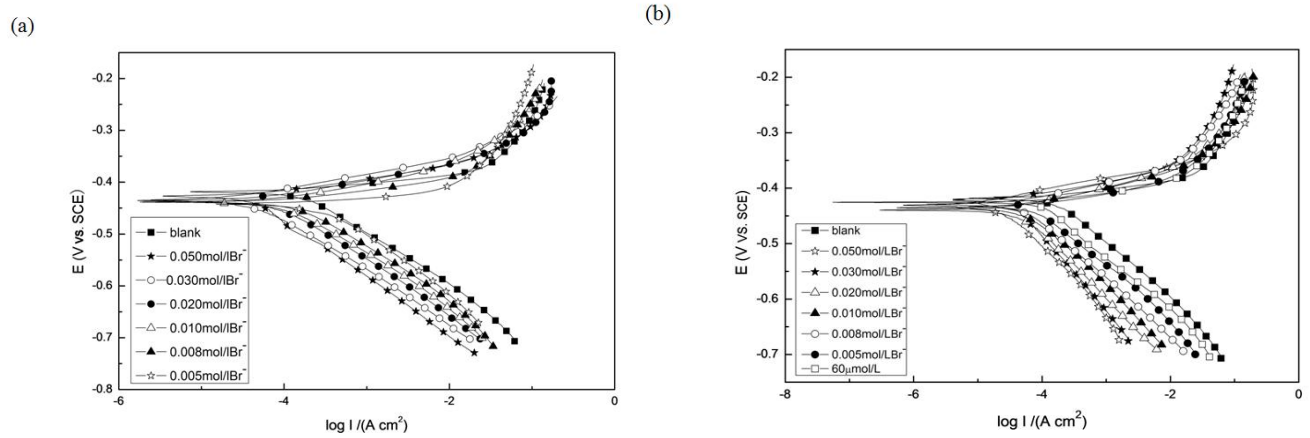

Figure 3. Polarization curves for mild steel in 0.5 mol/L H_2SO_4 containing different concentrations of Br^- in the absence (a) and presence (b) of 60 μmol/L PAN at 30 °C.

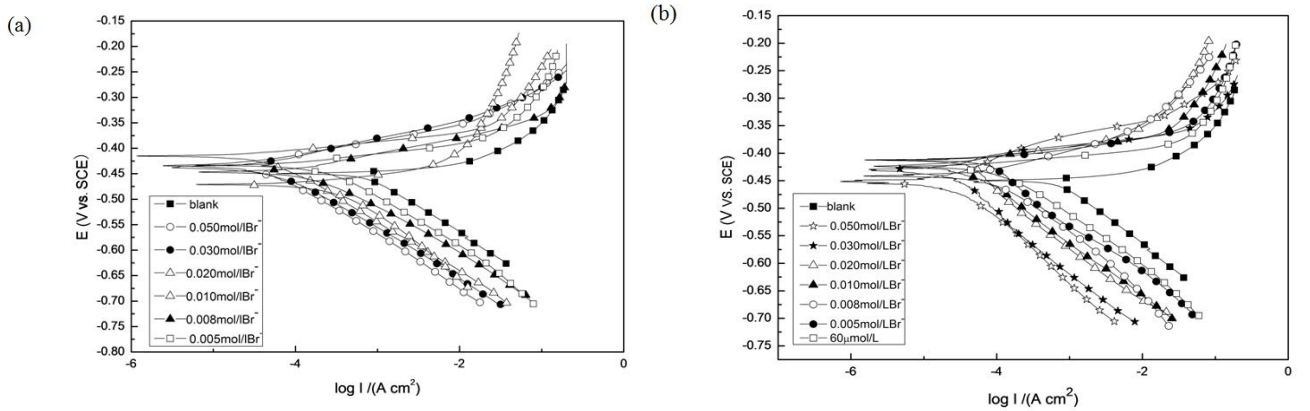

Figure 4. Polarization curves for mild steel in 0.5 mol/L H_2SO_4 containing different concentrations of Br^- in the absence (a) and presence (b) of 60 μmol/L PAN at 40 °C.

The potentiodynamic polarization parameters including corrosion current density (I_{corr}), corrosion potential (E_{corr}), anodic Tafel slope (β_a) and cathodic Tafel slope (β_c) values as functions of Br^- concentration in the presence and absence of PAN were obtained by Tafel plots and given in Table 1. β_a and β_c values do not show significantly changes and there is no regular change in the slopes of the

Tafel lines by changing the Br^- concentrations in the presence or absence of PAN, which indicates that the cathodic (hydrogen evolution) and anodic (steel dissolution) corrosion reaction mechanisms do not change[9,41]. It appears that inhibition occurred by a blocking mechanism on the available metal active centers [41,42]. Comparing the values of I_{corr} and *IE* of Br^- in the presence of PAN with those in the absence of PAN, decreases of corrosion current densities and improvements in inhibition efficiencies are distinctly observed in the presence of PAN. For instance, the highest *IE* is 62.3% only in the presence of Br^- and single PAN (60 μmol/L) also can not show so well inhibition efficiency. The highest *IE* of the complex (Br^- and PAN) has reached to 93.6%, meaning that the complex of Br^- and PAN is effective inhibitor for the corrosion of mild steel in 0.5 mol/L H_2SO_4 solution.

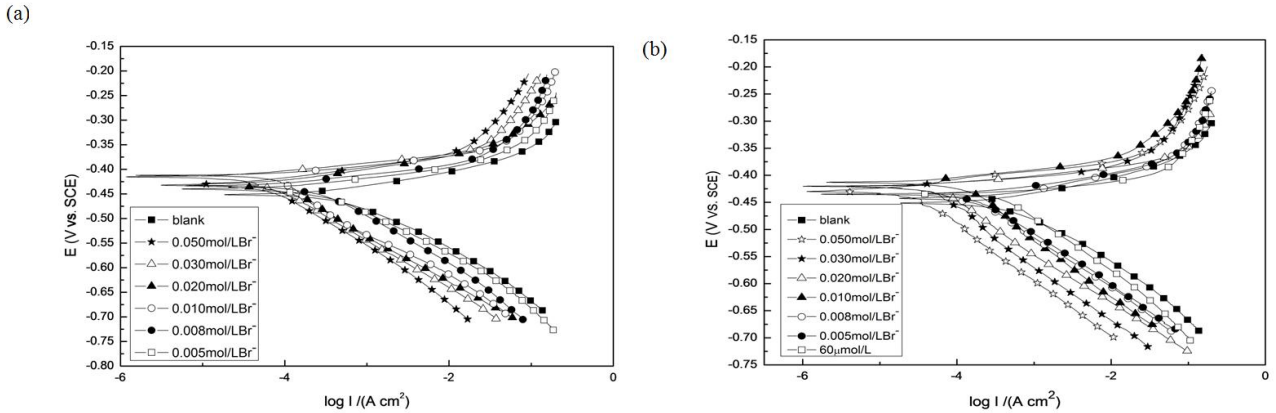

Figure 5. Polarization curves for mild steel in 0.5 mol/L H_2SO_4 containing different concentrations of Br^- in the absence (a) and presence (b) of 60 μmol/L PAN at 50 °C.

Table 2. Tafel polarization parameters and inhibition efficiencies for mild steel in 0.5 mol/L H_2SO_4 in the absence and presence of different concentration of inhibitors at 30 °C.

Br^- (mol/L)	PAN (μmol/L)	$-E_{corr}$ (vs SCE) (mv)	I_{corr} ($\mu A/cm^2$)	$-\beta_c$ (mV/dec)	β_a (mV/dec)	IE (%)
0	0	423.4	388.1	93.88	50.29	-
0.005	0	440.2	259.9	102.8	41.27	33.2
0.008	0	441.3	252.3	101.0	43.38	35.0
0.01	0	425.4	244.1	88.98	49.27	37.1
0.02	0	428.5	232.3	124.2	34.35	40.1
0.03	0	442.2	230.1	131.0	33.81	40.7
0.05	0	434.1	177.4	108.4	38.47	54.3
0	60	421.4	221.2	102.3	36.61	43.0
0.005	60	425.4	92.10	107.6	32.44	76.3
0.008	60	439.5	84.00	102.0	52.48	78.4
0.01	60	444.6	74.10	101.5	44.42	80.9
0.02	60	446.4	61.30	121.5	33.67	84.2
0.03	60	423.6	50.60	96.39	56.90	87.0
0.05	60	432.8	37.00	89.00	45.34	90.0

Table 3. Tafel polarization parameters and inhibition efficiencies for mild steel in 0.5 mol/L H_2SO_4 in the absence and presence of different concentration of inhibitors at 40°C.

Br^- (mol/L)	PAN (μmol/L)	$-E_{corr}$ (vs SCE) (mv)	I_{corr} ($\mu A/cm^2$)	$-\beta_c$ (mV/dec)	β_a (mV/dec)	IE (%)
0	0	449.1	443.5	95.88	52.29	-
0.005	0	435.2	326.9	101.8	43.37	26.3
0.008	0	447.9	322.4	100.0	44.38	27.3
0.01	0	472.3	321.6	87.80	50.30	27.5
0.02	0	417.5	312.7	121.2	36.53	29.5
0.03	0	441.3	301.1	129.0	34.81	32.1
0.05	0	437.9	243.4	107.1	39.57	45.2
0	60	424.3	251.9	113.9	37.38	40.2
0.005	60	411.5	146.9	105.7	33.54	66.8
0.008	60	441.3	138.4	102.8	52.48	68.8
0.01	60	426.3	134.7	100.5	46.42	69.6
0.02	60	424.3	117.1	111.7	31.67	73.6
0.03	60	443.7	101.7	95.40	55.90	77.1
0.05	60	451.8	59.80	90.21	47.24	86.5

Table 4. Tafel polarization parameters and inhibition efficiencies for mild steel in 0.5 mol/L H_2SO_4 in the absence and presence of different concentration of inhibitors at 50°C.

Br^- (mol/L)	PAN (μmol/L)	$-E_{corr}$ (vs SCE) (mv)	I_{corr} ($\mu A/cm^2$)	$-\beta_c$ (mV/dec)	β_a (mV/dec)	IE (%)
0	0	450.9	532.4	103.8	54.89	-
0.005	0	443.5	403.0	103.7	36.57	24.3
0.008	0	442.8	398.3	101.0	65.23	25.2
0.01	0	414.3	395.4	90.98	43.25	25.7
0.02	0	441.7	385.9	104.5	37.32	27.5
0.03	0	417.8	367.9	121.0	63.82	30.9
0.05	0	409.1	325.4	107.5	31.43	38.9
0	60	438.2	271.9	121.0	35.30	38.4
0.005	60	435.6	198.6	105.6	37.41	62.7
0.008	60	440.3	184.0	105.1	32.43	65.4
0.01	60	411.5	177.7	100.7	45.41	66.6
0.02	60	421.0	151.6	141.5	33.64	71.5
0.03	60	421.8	139.7	99.39	43.93	73.8
0.05	60	432.7	92.60	104.0	43.34	82.6

The effect of temperature on the inhibited acid–metal reaction is important and complicated [43]. The changes of the mild steel corrosion at different concentration of Br^- with the temperature were also studied in the absence and presence of PAN in 0.5mol/L H_2SO_4. The polarization readings at 30 ^oC, 40 ^oC, 50 ^oC were performed in Figure 3, Figure 4 and Figure 5, respectively. The corresponding potentiodynamic polarization parameters were given in Table 2, Table 3 and Table 4 too. It is obvious that the values of I_{corr} increase and the *IE* decreases gradually by increasing in temperature at same concentration of Br^- in the absence and presence of PAN. Raising the temperature has no significant effect on the corrosion potentials, but leads to a higher corrosion rate (I_{corr}). At the same time it also can be seen that the *IE* increases gradually with increasing Br^- concentration in the absence and presence of PAN at each experimental temperature. These results indicate the inhibition of the inhibitors for steel corrosion might be caused by the adsorption of the inhibitors on the steel surface. However at higher temperature, the desorption of the inhibitors from the steel surface might be taken place. However, the combination of Br^- and PAN still can show more effective inhibition than single Br^- at experimental temperatures.

3.2. Adsorption isotherm

Assuming the corrosion inhibition was caused by the adsorption of Br^- or PAN on the steel surface and the Langmuir adsorption isotherm was applied to investigate the adsorption mechanism by following equation [44]:

$$\frac{C}{\theta} = \frac{1}{K_{ads}} + C \qquad (2)$$

where C is the concentration of the inhibitor, θ is the surface coverage by inhibitor molecules and K_{ads} is the adsorptive equilibrium constant.

Figure 6 is the relationship between C/θ and C in the absence (a) and presence (b) of PAN in 0.5 mol/L H_2SO_4 solution. Table 5 shows the corresponding parameters obtained.

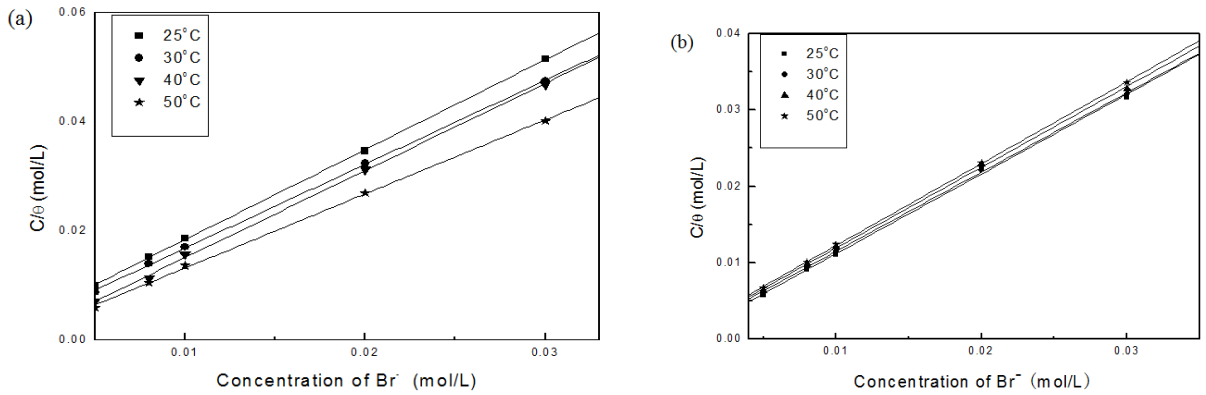

Figure 6. *C/θ–C* curves for different concentrations of Br^- in the absence (a) and presence (b) of 60 μmol/L PAN in 0.5 mol/L H_2SO_4 solution.

Table 5. Langmuir isotherm parameters for Br^- adsorbed on the mild steel surface in the absence and presence of 60 μmol/L PAN.

Inhibitor	Temperature (℃)	Linear regression Coefficient (R^2)	slope	K_{ads} ($\times 10^4$ L/mol)
Br^-	25	0.9998	1.648	0.526
Br^-	30	0.9997	1.538	0.714
Br^-	40	0.9983	1.515	1.110
Br^-	50	0.9994	1.357	2.500
Br^- + PAN	25	0.9988	1.045	8.428
Br^- + PAN	30	0.9997	1.039	7.100
Br^- + PAN	40	0.9939	1.059	5.769
Br^- + PAN	50	0.9932	1.073	3.667

Obviously, the R^2 values are very close to unity, indicating that the adsorption of Br^- on the mild steel surface in the absence and presence of PAN obeys the Langmuir adsorption isotherm. From the Table 5, it can be seen that the value of K_{ads} is very large to 10^4, which means the trend of adsorption of Br^- onto the steel surface is strong. Compared the values of K_{ads} measured in the presence and absence of 60 μmol/L PAN, it is found that the values of K_{ads} are larger in the presence of PAN than the absence, which means the trend of adsorption of combination of $Br^-$and PAN is stronger than single presence of Br^-.

3.3. Thermodynamic parameters

Thermodynamic model is very useful to explain the adsorption phenomenon of inhibitor. According to the Van't Hoff equation [45]:

$$\ln K_{ads} = \frac{-\Delta H^{\circ}_{ads}}{RT} + B \qquad (3)$$

where ΔH^{o}_{ads} is the standard adsorption heat. T is the absolute temperature, B is a constant. Clearly, from the equation 3 the adsorption heat can be obtained by the slope of the regression.

To obtain the standard adsorption free energy (ΔG^{o}_{ads}), the following equation was used [46-47]:

$$K_{ads} = \frac{1}{55.5}\exp(\frac{-\Delta G^{\circ}_{ads}}{RT}) \qquad (4)$$

where the value 55.5 is the molar concentration of water in solution in mol/L. The standard adsorption entropy (ΔS^{o}_{ads}) could also be obtained from the basic thermodynamic equation 5

$$\Delta G^{o}_{ads} = \Delta H^{o}_{ads} - T\Delta S^{o}_{ads} \qquad (5)$$

Table 6 gives the thermodynamic parameters calculated. In the absence of 60 μmol/L PAN the positive values of ΔH^{o}_{ads} indicate that it is an endothermic process that the bromide ions were adsorbed on the mild steel surface. With the addition of 60 μmol/L PAN the values of ΔH^{o}_{ads} are negative, which suggests that the adsorption of the combination of bromide ions and PAN is an exothermic process.

Table 6. Some thermodynamic data for Br^- and PAN adsorbed on the mild steel surface at experimental temperatures.

Inhibitor	Temperature (℃)	ΔG^o_{ads} (kJ/mol)	ΔH^o_{ads} (kJ/mol)	ΔS^o_{ads} (J/mol K)
Br^-	25	-31.19	48.49	267.2
Br^-	30	-32.49	48.49	267.1
Br^-	40	-34.71	48.49	265.7
Br^-	50	-38.00	48.49	267.7
Br^- + PAN	25	-38.10	-24.44	45.60
Br^- + PAN	30	-38.28	-24.44	45.65
Br^- + PAN	40	-39.00	-24.44	46.50
Br^- + PAN	50	-39.03	-24.44	45.15

Generally, values of ΔG^o_{ads} around 20 kJ/mol or lower are consistent with the electrostatic interaction between the charged molecules and the charged metal (physisorption), while those more negative than -40 kJ/mol involve charge sharing or transfer from the inhibitor molecules to the metal surface to form a coordinate type of bond (chemisorption) [43,48]. The calculated ΔG^o_{ads} values for Br^- in the absence or presence of PAN show that adsorption mechanism is not completely physical or chemical adsorption and a combination of physisorption and chemisorption exists between the inhibitors and metal surface [44,49]. It is also clear that the chemisorption is the dominant in the presence of PAN. The high negatively ΔG^o_{ads} values may be attributed to the tightly adsorbed inhibitor molecules on the metal-solution interface [50-51].

Without addition of PAN the positive values of ΔS^o_{ads} indicate that the adsorption is a process accompanied by an increase in entropy. The increase of entropy is the main driving force of spontaneous process bromide ions adsorbed on the steel surface (positive ΔH^o_{ads} values). When in the presence of PAN negative ΔH^o_{ads} and increase of entropy shows that the exothermic and the increase of entropy is the main driving force of spontaneous process Br^- and PAN adsorbed on the steel surface. The positive sign of ΔS^o_{ads} arises from substitutional process, which can be attributed to the increase in the solvent entropy and more positive water desorption entropy [15]. It also interpreted with increase of disorders due to the more water molecules which can be desorbed from the metal surface by one inhibitor molecule [15,52].

3.4. Kinetic parameters

The values of the apparent activation energy of the corrosion process in H_2SO_4 solution was calculated using the Arrenius equation:

$$\ln I_{corr} = \frac{-E_a}{RT} + \ln A \qquad (6)$$

where E_a is apparent activation energy, R is universal gas constant, and A is pre-exponential factor.

Equation 6 is shown graphically in Figure. 7 without (a) and with (b) PAN, respectively.

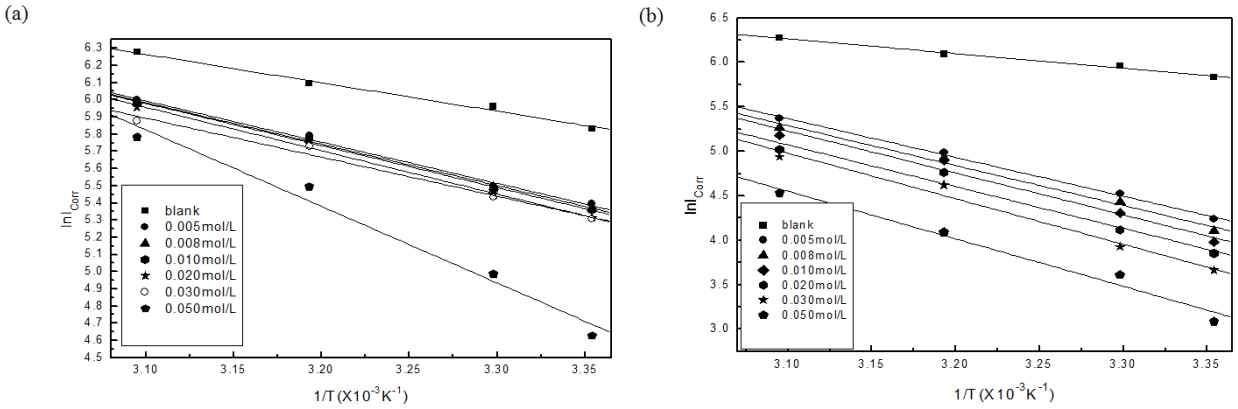

Figure 7. The relationship between lnI_{corr} and 1/T without (a) and with (b) 60 μmol/L PAN at different temperature.

Table 7. Parameters of the linear regression between lnI_{corr} and 1/T.

Br^- (mol/L)	PAN (μmol/L)	E_a (kJ/mol)	Pre-exponential factor A ($\times 10^5$ g/cm^{2}h)	Linear regression Coefficient(R^2)
0	0	43.7	0.884	0.9906
0.005	0	49.9	6.81	0.9953
0.008	0	50.1	7.06	0.9979
0.01	0	50.3	7.74	0.9966
0.02	0	50.9	9.59	0.9968
0.03	0	58.8	4.15	0.9848
0.05	0	61.0	33.3	0.9786
0.005	60	56.2	156	0.9970
0.008	60	57.3	219	0.9895
0.01	60	59.2	417	0.9771
0.02	60	69.0	330	0.9739
0.03	60	72.6	1150	0.9808
0.05	60	74.3	1460	0.9749

E_a and A at different concentrations of Br^- were calculated by liner regression between ln I_{corr} and *1/T* and the results are given in Table 7.

It is reported that higher value of E_a in the presence of inhibitor for steel in comparison with blank solution was considered as physisorption that occurred in the first stage by forming an adsorptive film of an electrostatic character on steel surface [44,53]. Because the electrochemical corrosion is relevant to heterogeneous reactions, the pre-exponential factor A in the Arrhenius equation is related to

the number of active centers. There are two possibilities about these active centers with different E_a on the metal surface: (1) the activation energy in the presence of inhibitor is higher than that of pure acidic medium, which shows the inhibitor adsorbed on most active adsorption sites (having the lowest energy) and the corrosion takes place chiefly on the active sites (having higher energy); (2) the activation energy in the presence of inhibitors is lower than that of pure acidic medium, which suggests a smaller number of more active sites remain uncovered in the corrosion process.

The apparent activation energy acts as a function of concentration of Br^- from the Table 7. The values of E_a in the presence of single Br^- or Br^-+PAN are higher than that in the uninhibited acid solution and increase with elevating the concentration of Br^-. So, it is clear that the adsorption of Br^- or Br^-+PAN on mild steel surface blocks the active sites from acid solution and consequently increases the apparent activation energy.

According to Eq.6, it is evident that the I_{corr} is controlled by E_a and A at a certain temperature. It is also clear that effect of E_a on steel corrosion is larger than that of A, which suggests that E_a is the mainly deciding factor for decrease of steel corrosion rate by increasing inhibitor concentration. It is also seen that the E_a increased in the presence of PAN in comparison to the without addition of PAN. The increases of the apparent activation energy decrease further the steel corrosion rate in the coexistence of Br^- and PAN.

3.5. Electrochemical impedance spectroscopy

Figure 8 shows Nyquist plots of mild steel in 0.5 mol/L H_2SO_4 solutions for Br^- without (a) and with (b) 60 μmol/L PAN at 25 ^oC, respectively.

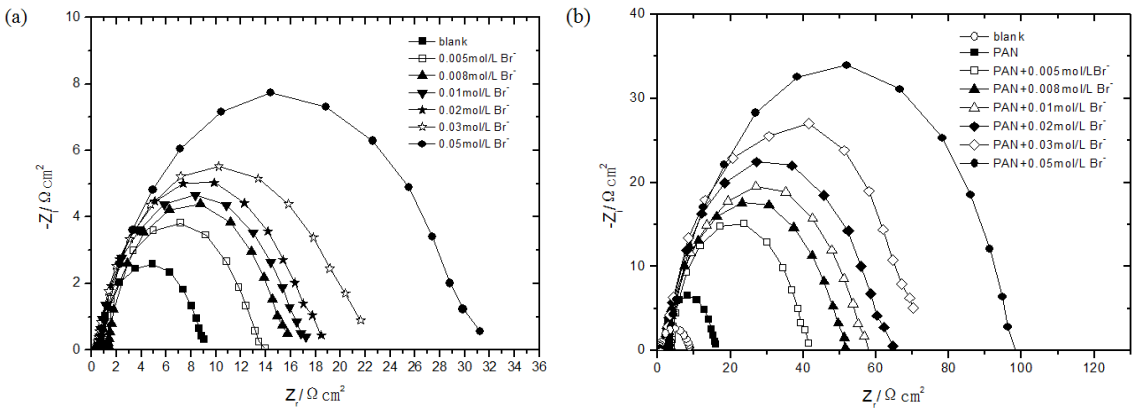

Figure 8. EIS for mild steel in 0.5 mol/L H_2SO_4 containing different concentrations of Br^- in the absence (a) and presence (b) of 60 μmol/L PAN at 25 ^oC.

It is clear that all Nyquist impedance plots in the absence or presence inhibitors in H_2SO_4 solution show a single capacitive loop of characteristic depressed semicircles which is related to charge transfer of the corrosion process. These results indicate that the corrosion inhibition of mild steel is controlled predominantly by a charge transfer process and the mechanism of steel dissolution is not changed in the presence of inhibitor [54]. The imperfect semicircles presented in Figure 8 are related to the frequency dispersion due to the roughness and in-homogeneity of electrode surface

[54,55]. Comparing the capacitive loops in the absence of PAN with those without PAN, it is seen that the diameters of the semicircles with PAN are bigger than those without PAN, meaning that PAN can effectively promote anti-corrosion performance of Br^-.

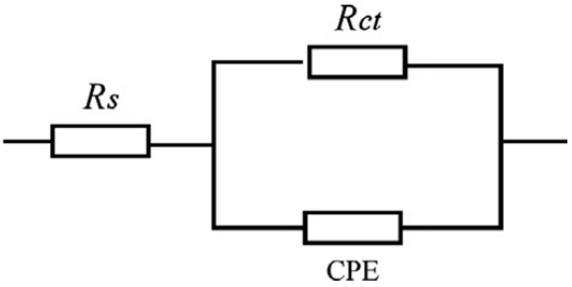

Figure 9. Equivalent circuit model used to fit the EIS experiment data.

The EIS results were simulated by the equivalent circuit shown in Figure 9 to pure electronic models that could verify the mechanistic models and enable the calculation of numerical values corresponding to the physical and/or chemical properties of the tested electrochemical system [56-57]. In this equivalent circuit, the electrochemical impedance parameters such as solution resistance (R_S), charge transfer resistance (R_{ct}) and the double layer capacitance (C_{dl}) were obtained. It is clear that C_{dl} value is influenced by the surface roughness, and this effect is simulated through a constant phase element (CPE) [56]. The CPE is composed of a component Q_{dl} and a coefficient α which quantifies different physical phenomena like surface inhomogeneous resulting from surface roughness, inhibitor adsorption, porous layer formation, etc. So C_{dl} can be calculated by the following expression [30]:

$$C_{dl} = Q_{dl} \cdot (2\pi f_{max})^{\alpha-1} \qquad (7)$$

Where f_{max} represents the frequency at which the imaginary part of the impedance is maximum. If the electrode surface is homogeneous and plane, $\alpha = 1$, and the electrode surface can be treated as an ideal capacitance. Parametrical adjustment of this circuit with experimental impedance spectra gives access to the double layer capacitance and charge transfer resistance.

The inhibition efficiency values of the inhibitor can also be calculated from the data of EIS through the use of following equation:

$$IE_t = \frac{R_{ct(inh)} - R_{ct(0)}}{R_{ct(inh)}} \times 100 \qquad (8)$$

where $R_{ct(inh)}$ and $R_{ct(0)}$ are the charge-transfer resistances in the presence and absence of inhibitor, respectively. The impedance parameters of R_{ct}, R_s, C_{dl} and IE_{ct} are given in Table 8.

As can be seen from Table 8, the values of R_{ct} increase and the values of C_{dl} values decrease to some extent with increasing concentration of Br^- without addition of PAN, as a result, the inhibition efficiencies also increase to a certain extent, which means that corrosion of mild steel can be inhibited somewhat by single Br^- but the corrosion inhibition is limited. However the addition of 60 μmol/L PAN to 0.5 mol/L H_2SO_4 containing Br^- further enhances values of R_{ct} and reduces values of C_{dl}, and the inhibition efficiencies increase clearly. These results are in good agreement with that by Tafel polarization curves.

Table 8. Impedance data obtained for mild steel in 0.5 mol/L H_2SO_4 in absence and presence of different concentrations of Br^- at 25 ^oC.

Br^- (mol/L)	PAN (μmol/L)	R_s (Ω cm^2)	C_{dl} ($\mu F/cm^2$)	R_{ct} (Ω cm^2)	IE (%)
0	0	0.7328	817.1	7.752	-
0.005	0	0.4347	795.2	11.56	32.9
0.008	0	0.5556	735.6	12.43	37.6
0.01	0	0.6371	701.2	13.49	42.5
0.02	0	0.4778	643.7	14.55	46.7
0.03	0	0.7801	635.5	16.93	54.2
0.05	0	0.6587	601.1	24.55	68.4
0	60	0.8144	705.8	13.47	42.4
0.005	60	0.9874	535.5	34.29	77.4
0.008	60	0.8562	520.9	43.73	82.3
0.01	60	0.6142	501.8	48.59	84.0
0.02	60	0.5789	466.4	54.43	85.7
0.03	60	0.6574	453.1	61.62	87.4
0.05	60	0.5748	406.3	83.41	90.7

3.6. Weight loss measurements

Table 9. Inhibition efficiencies obtained from weight less for mild steel in 0.5 mol/L H_2SO_4 at 25 and 40℃.

Br^- (mol/L)	PAN (μmol/L)	IE（%） 25℃	40℃
0	0		
0.005	0	37.4	27.2
0.008	0	38.2	28.3
0.01	0	39.3	29.4
0.02	0	41.5	30.7
0.03	0	44.1	34.1
0.05	0	65.1	47.3
0	60	46.2	41.2
0.005	60	83.9	68.9
0.008	60	84.5	69.8
0.01	60	85.6	71.4
0.02	60	87.8	75.4
0.03	60	90.5	78.9
0.05	60	95.4	88.8

The inhibition efficiency values obtained from weight loss measurements for different concentrations of Br^- in 0.5 mol/L H_2SO_4 solutions in the absence and presence of 60 μmol/L PAN are presented in Table 9. The inhibition efficiency (*IE*) is determined by the following relation:

$$IE = \frac{V_0 - V_i}{V_0} \times 100 \qquad (9)$$

where V_0 and V_i are the weight losses per unit area per unit time in the absence and presence of the inhibitor, respectively.

As seen, the *IE* increases gradually with increasing Br^- concentration in the absence and presence of PAN. It is also very clear that the inhibition efficiency of the combination of Br^- and PAN is quietly improved compared with the only in the presence of single Br^- or PAN and the *IE* decreases gradually by increasing in temperature at same concentration of Br^- in the absence and presence of PAN, which is similar to those obtained from polarization measurements

3.7. Synergism parameter

The studies reveal that the inhibition efficiencies for solutions with Br^- and PAN exhibit higher values compared to solutions only with Br^-, which means that PAN may have a synergistic inhibitive effect on the mild corrosion in H_2SO_4 media. The synergistic inhibition effect of inhibitors takes place when the total action of compounds is higher than the sum of each one individually. The synergism parameters (S) were calculated using the following equation [58]:

$$S = \frac{1-(IE_1 + IE_2)}{1-IE_{1+2}} \qquad (10)$$

where IE_{1+2} is the inhibition efficiency of inhibitor 1 + 2 mixture, IE_1 is the inhibition efficiency of inhibitor 1 and IE_2 is the inhibition efficiency of inhibitor 2.

Table 10. Synergism parameters between Br^- and PAN in 0.5 mol/L H_2SO_4 at testing temperatures.

Br^- (mol/L)	PAN (μmol/L)	Synergism parameters(*S*)			
		25℃	30℃	40℃	50℃
0.005	60	1.078	1.004	1.009	1.000
0.008	60	1.011	1.019	1.042	1.052
0.01	60	1.089	1.042	1.062	1.075
0.02	60	1.029	1.070	1.148	1.196
0.03	60	1.210	1.254	1.210	1.172
0.05	60	-1.187	0.270	1.081	1.305

Generally, in the case of $S > 1$ synergistic interaction of two inhibitors prevails. While $S < 1$, the antagonistic behavior exits between two inhibitors, indicating that there is a competitive adsorption, [59]. The values of *S* were calculated by Eq. (10) and shown in Table 10. It is noticed that almost all of the values of *S* are great than unity from the table, which suggests that the improvement in inhibition efficiency is due to a synergistic effect generated by the addition of PAN to H_2SO_4 containing Br^-.

3.8. Mechanism of synergistic inhibition

From the chemical structure of PAN, it is clearly seen that PAN is an organic compound containing heteroatom-nitrogen, lone-pair electrons and π-electrons. It would be protonated in the H_2SO_4 solution as following:

$$PAN + xH^+ \rightarrow [PANH_x]^{x+} \quad (11)$$

The charge of the metal surface can be determined from the value of $E_{corr}–E_{q=0}$ (zero charge potential (vs. SCE)) [60]. The $E_{q=0}$ of iron is –550 mV versus SCE in H_2SO_4 [61]. In the present wok, it is known that the steel surface contains positive charge because of $E_{corr}–E_{q=0} > 0$ compared with the value of E_{corr} obtained in 0.5 mol/L H_2SO_4 versus SCE. So the positively charged PAN is not easy to be adsorbed directly on the positively charged surface of mild steel as a result of the electrostatic repulsion, which gives the explanation that the inhibition of single PAN for the steel corrosion is not so excellent in H_2SO_4 solution. In the coexistence of Br^- and PAN in H_2SO_4 solution, since the bromide anions adsorb specifically on the steel surface, they create an excess negative charge exposed to the solution and favor more adsorption of the PAN cations due to the electrostatic influence (physical adsorption) between Br^- and PAN. Further, the donor-acceptor interaction between the π-electrons or nitrogen atom and the vacant d-orbital of surface iron atoms (chemical adsorption) could occur.

4. CONCLUSION

(1) Single Br^- or PAN can inhibit the corrosion of mild steel in 0.5 mol/L H_2SO_4, but the inhibition efficiency is not satisfactory. The inhibition efficiency of the combination of Br^- and PAN is enormously increased, indicating a synergistic inhibition effect exists between Br^- and PAN for mild steel corrosion in H_2SO_4 solution.

(2) Single Br^- acts as a mixed type inhibitor inhibiting the corrosion at both cathode and anode at same time for mild steel in 0.5 mol/L H_2SO_4 solution. The combination of Br^- and PAN acts as a mixed type inhibitor too. The inhibitors reduce anodic steel dissolution and retard cathodic hydrogen evolution reaction by blocking the active reaction centers on the steel surface.

(3) The adsorption mode of Br^- on the surface of mild steel without and with PAN obeys the Langmuir adsorption isotherm. The values of ΔG^o_{ads} indicate that the adsorption of the inhibitor is a spontaneous process and show a combination of physical and chemical adsorption. The chemisorption is the dominant in the presence of Br^- and PAN together.

(4) Electrochemical impedance spectroscopy shows that the fact the corrosion reaction is controlled by charge transfer. The outcomes from electrochemical methods are in good agreement with that by weight loss.

ACKNOWLEDGEMENT
This work was financially supported by the National Natural Science Foundation of China under the Grant No. 51161025

References

1. L. Guo, S.T. Zhang, W.P. Li, G. Hu and X. Li, *Mater. Corros.*, 65 **(**2014) 935.
2. N. Sato, *Corros. Sci*., 27 (1987) 421.
3. Y.A. Albrimi, A.A. Addi, J. Douch, M. Hamdani and R.M. Souto, *Int. J. Electrochem. Sci*., 11 (2016) 385.
4. M. Farsak, H. Keleş and M. Keleş, *Corros. Sci.*, 98 (2015**)** 223.
5. M.J. Banera, J.A. Caram, C.A. Gervasi and M.V. Mirífico, *J. Appl. Electrochem.*, 44 (2014) 1337.
6. G. Trabanelli, *Corrosion*, 47 (1991) 410.
7. P. Thanapackiam, S. Rameshkumar, S.S. Subramanian and K. Mallaiya, *Mater. Chem. Phys.*, 174 (2016) 129.
8. G. Žerjav and I. Milošev, *Corros. Sci.*, 98 (2015) 180.
9. A.A. Farag and M.A. Hegazy, *Corros. Sci.*, 74 (2013) 168.
10. A.Y. Musa, A.B. Mohamad, A.A.H. Kadhum and M.S. Takriff, *Int. J. Electrochem. Sci*., 6 (2011) 2758.
11. T. Kosec, I. Milošev and B. Pihlar, *Appl. Surf. Sci.*, 253 (2007) 8863.
12. L. Wang, *Corros.. Sci.*, 48 (2006) 608.
13. R.Y. Khaled, A.M. Abdel-Gaber and H.M. Holail, *Int. J. Electrochem. Sci*., 11 (2016) 2790.
14. A. M. Al-Bonayan, *Int. J. Electrochem. Sci*., 10 (2015) 589.
15. R. Solmaz, G. Kardaş, M. Çulha, B. Yazici and M. Erbil, *Electrochim. Acta*, 53 (2008) 5941.
16. L. Wang, J.X. Pu and H.C. Luo, *Corros. Sci.*, 45 (2003) 677.
17. L.A. Al Juhaiman, *Int. J. Electrochem. Sci*., 11 (2016) 2247.
18. G. Moretti, F. Guidi and F. Fabris, *Corros. Sci.*, 76 (2013) 206.
19. S.K. Shukla and E.E. Ebenso, *Int. J. Electrochem. Sci*., 6 (2011) 3277.
20. R. Salghi, D.B. Hmamou, E. E. Ebenso, O. Benali, A. Zarrouk and B. Hammouti, *Int. J. Electrochem. Sci*., 10 (2015) 259.
21. R. Yıldız, T. Doğan and I. Dehri, *Corros. Sci.*, 85 (2014) 215.
22. S. Liu, W.W. Guan, Y.H. Yan, R.Y. Jiang, Z.P. Feng, W.J. Song and K. Qin, *Mater. Corros.*, 64 (2013) 932.
23. Sh. Pournazari, M.H. Moayed and M. Rahimizadeh, *Corros. Sci.*, 71 (2013) 20.
24. R.Y. Khaled, A.M. Abdel-Gaber and H.M. Holail, *Int. J. Electrochem. Sci*., 11 (2016) 2790.
25. R. Yıldız, *Corros. Sci.*, 90 (2015) 544.
26. S.M.A. Hosseini, M.J. Bahrami and A. Dorehgiraee, *Mater. Corros.*, 63 (2012) 627.
27. N. Caliskan and E. Akbas, *Chem. Phys.*, 126 (2011) 983.
28. S. Zhang, Z. Tao, W. Li and B. Hou, *Appl. Surf. Sci.*, 255 (2009) 6757.
29. F. Bentiss, M. Traisnel, N. Chaibi, B. Mernari, H. Vezin and M. Lagrenée, *Corros. Sci.*, 44 (2002) 2271.
30. M. Lagrenée, B. Mernari, M. Bouanis, M. Traisnel and F. Bentiss, *Corros. Sci.*, 44 (2002) 573.
31. R. Fuchs-Godec and M.G. Pavlović, *Corros. Sci.*,58 (2012) 192.
32. X. Wang, H. Yang and F. Wang, , *Corros. Sci.*, 55 (2012) 145.
33. L. Tang, X. Li, G. Mu and L. Li, *Appl. Surf. Sci.*, 252 (2006) 6394.
34. G. Moretti, F. Guidi and F. Fabris, *Corros. Sci.*, 76 (2013) 206.
35. L. Wang, F.C. Yang, J. Ma, Z.W. Fang, S.W. Zhang and Q. Guo, *Asian J. Chem.*, 25 (2013) 10305.
36. L. Tang, X. Li, L. Li, G. Mu and G. Liu, *Mater. Chem. Phys.*, 97 (2006) 301.
37. G. Mu,. X. Li and F. Li, *Mater. Chem. Phys.*, 86 (2004) 59.
38. H. Amar, J. Benzakour, A. Derja, D. Villemin and B. Moreau, *Corros. Sci.*, 50 (2008) 124.
39. L. Qiu, Y. Wu, Y. Wang and X. Jiang, *Corros. Sci.*, 50 (2008) 576-582.
40. M, El Achouri, M,S, Infante, F, Izauierdo, S. Kertit, H.M. Gouttaya, B. Nciri, *Corros. Sci.*, 43 (2001) 19.
41. N.A. Negm, F.M. Ghuiba and S.M. Tawfik, *Corros. Sci.*, 53 (2011) 3566.

42. K.C. Emregül and M. Hayvalí, *Corros. Sci.*, 48 (2006) 97.
43. F. Bentiss, M. Lebrini and M. Lagrenée, *Corros. Sci.*, 47 (2005) 2915.
44. E.A. Noor and A.H. Al-Moubaraki, *Mater. Chem. Phys.*, 110 (2008) 145.
45. M.A. Migahed, M.A. Hegazy and A.M. Al-Sabagh, *Corros. Sci.*, 61 (2012) 10.
46. E. Cano, J.L. Polo, A.L.A. Iglesia and J.M. Bastidas, *Adsorption*, 10 (2004) 219.
47. E. Khamis, *Corrosion*, 46 (1990) 476.
48. E. Machnikova, K.H. Whitmire and N. Hackerman, *Electrochim. Acta*, 53 (2008) 6024.
49. M.A. Hegazy and M.F. Zaky, *Corros. Sci.*, 52 (2010) 1333.
50. M.B. Valcarce and M. Vazquez, *Mater. Chem. Phys.*, 115 (2009) 313.
51. S.A. Ali, H.A. Al-Muallem, M.T. Saeed and S.U. Rahman, *Corros. Sci.*, 50 (2008) 664.
52. G. Avci, *Colloid Surf. A*, 317 (2008) 730.
53. A, Popova, E, Sokolova, S, Raicheva and M, Christov, *Corros. Sci.*, 45 (2003) 33.
54. M. Lebrini, M. Lagrenée, H. Vezin, M. Traisnel and F. Bentiss, *Corros. Sci.*, 49 (2007) 2254.
55. N. Labjar, M. Lebrini, F. Bentiss, N.E. Chihib, S. El Hajjaji and C. Jama, *Mater. Chem. Phys.*, 119 (2010) 330.
56. P. Bommersbach, C. Alemany-Dumont, J.P. Millet and B. Normand, *Electrochim. Acta*, 51 (2006) 4011.
57. S.E. Nataraja, T.V. Venkatesha, K. Manjunatha, B. Poojary, M.K. Pavithra and H.C. Tandon, *Corros. Sci.*, 53 (2011) 2651.
58. L. Larabi, Y. Harek, M. Traisnel and A. Mansri, *J. Appl. Electrochem.*, 34 (2004) 833.
59. S.A. Umoren, O. Ogbobe, I.O. Igwe and E..E. Ebenso, *Corros. Sci.*, 50 (2008) 1998.
60. D.P. Schweinsberg and V. Ashworth, *Corros. Sci.*, 28 (1988) 539.
61. S.C. Roy, S.K. Roy and S.C. Sircar, *Br. Corros. J.*, 32 (1988) 102.